ICARUS **120,** 358–370 (1996)
ARTICLE NO. 0056

Mean-Motion Resonances as a Source for Infalling Comets toward β Pictoris

HERVÉ BEUST

Observatoire de Grenoble, Université J. Fourier, B.P. 53, F-38041 Grenoble Cedex 9, France
E-mail: beust@gag.observ-gr.fr

AND

ALESSANDRO MORBIDELLI

Observatoire de la Côte d'Azur, Le Mont Gros, B.P. 229, F-06304 Nice Cedex 4, France

Received April 27, 1995; revised October 2, 1995

Repeated time-variable redshifted absorption features in the spectrum of β Pictoris (β Pic) have been attributed to comet-like bodies falling toward the star, when evaporating in its immediate vicinity. This model explains now a large number of observational characteristics, but the exact mechanism that could generate these numerous star-grazers is still controversial, even if planetary perturbations are thought to be the basic process. The different models proposed up to now are here reviewed, and we discuss in particular a recent one, involving the effect of secular resonances in the β Pic system. We stress that it seems highly improbable that such a mechanism could apply to the β Pic case, because the extremely strong power of secular resonances is connected to the very specific structure of the Solar System. Therefore, the secular resonance mechanism is highly non-generic. Conversely, we propose a model involving the eccentricity-pumping effect of mean-motion resonances with a massive planet on a moderately eccentric orbit. We show in particular that the 4 : 1 mean-motion resonance is a very active source of star-grazers as soon as the eccentricity of the perturbing planet is $\gtrsim$0.05, while the 3 : 1 mean-motion resonance is less efficient. We stress that this mechanism is very generic. These theoretical predictions are confirmed by numerical integrations using the Extended Schubart Integrator. The time-scale of the process is discussed, and we show that if the eccentricity of the perturbing planet fluctuates, due to secular perturbations, this time-scale is compatible with the age of β Pic's system. © 1996 Academic Press, Inc.

1. INTRODUCTION

The dusty and gaseous circumstellar disk around the southern star β Pictoris (β Pic) (Aumann *et al.* 1984, Smith and Terrile 1984; Paresce and Burrows 1987) is regarded today as an obvious candidate for an extra-solar planetary system. The age of β Pic is estimated at 2×10^8 yr at most (Paresce 1991), meaning that this system is probably much less evolved than the Solar System. The presence of large bodies, such as planets, within that disk is still controversial, but strongly suspected. First, theoretical arguments (Lissauer 1993) show that planetary systems are able to form within $\sim 10^7$–10^8 yr. Second, various observational features are regarded as indirect clues for the presence of planets orbiting β Pic: (i) the radial variations of the optical properties of grains (Golimowski *et al.* 1993; Lecavelier *et al.* 1993); (ii) the strong cut-offs in the radial distribution of grains at $\sim$20 AU from the star (Lagage and Pantin 1994); (iii) the disk asymmetries, which could be due to gaps or azimuthal dust confinement in the disk (Roques *et al.* 1994; Lazzaro *et al.* 1994).

The gaseous part of the disk around β Pic may also provide strong arguments in favor of the presence of hidden solid bodies. The favorable edge-on orientation of the disk enables the detection of absorption features due to the circumstellar gas in the spectral lines of the star. First seen in 1985 by Hobbs *et al.*, this phenomenon has been the subject of intense investigation in the past years. A large number of lines were observed to exhibit several temporally varying absorption features, which appeared or disappeared on time-scales on the order of a day or even less. These features are always redshifted by velocities ranging from a few tens to a few hundreds of km sec^{-1} with respect to the star (Kondo and Bruhweiler 1985; Grady *et al.* 1991; Boggess *et al.* 1991; Bruhweiler *et al.* 1991; Lagrange *et al.* 1995; Vidal-Madjar *et al.* 1994, and Refs. therein).

These repeated spectral events have been interpreted as the signature of the evaporation of kilometer-sized bodies in the vicinity of the star (Vidal-Madjar *et al.* 1994).

0019-1035/96 $18.00

Since the presumed bodies are moving toward the star, this model has been termed the falling evaporating body (FEB) scenario. This scenario has been extensively studied in the past years. Dynamical simulations reproduce the observed events in many of their characteristic details (Beust *et al.* 1990; Beust *et al.* 1995, and Refs. therein). Moreover, some very specific features related to the observed events, such as unusual line ratios or the unexpected presence of overionized species like Al III or C IV, appear to be a natural consequence of the physics implied by the scenario of comet (FEB) evaporation (Beust and Tagger 1993; Mouillet and Lagrange 1995). Conversely, these features would be hardly explained by any other model.

The estimated rate of events is on the order of several hundreds per year (Lagrange-Henri *et al.* 1992). Since theoretical models of the formation of our Solar System imply that the rate of cometary bombardment was also several orders of magnitude greater (Wetherill 1994) when the Solar System was at the age of β Pic (2×10^8 yr; Paresce 1991), such a frequency is compatible with this estimated age. However, the mechanism that could generate such a large infall of solid bodies toward the star is still controversial. A common idea is that planetary perturbations may be responsible for the phenomenon in various ways.

A simple approach was developed a few years ago (Beust *et al.* 1991), investigating the direct effect of close encounters of particles on circular orbits around the star with a single massive planet. It was shown that, unless the eccentricity of the planet is large enough ($\gtrsim$0.6), the perturbations were not efficient. However, such an eccentric orbit for a massive planet seems to be quite unrealistic.

We have also proposed (Beust and Lissauer 1994) that at least part of the FEBs could be members of a family, i.e., they could originate from the tidal break-up of a larger body initially on a star-grazing orbit. However, we showed (Beust *et al.* 1995) that the mere assumption of this model is not compatible with some observational characteristics, such as the periastron dispersion of the FEBs.

Another mechanism, involving a secular resonance corresponding to the ν_6 resonance in the Solar System (and thus requiring at least two planets orbiting β Pic) has been proposed recently (Levison *et al.* 1994). This model is compatible with a large amount of the observational data. Unfortunately, the efficiency of the ν_6 mechanism is intimately connected to the specific structure of our Solar System, so that it is unlikely that this mechanism would work in the β Pic disk.

On the other hand, recent calculations (Gor'kavyi and Taidakova 1995) investigating the dynamics of particles in the field of two planets in mean-motion resonance, under the random effect of close encounters, were able to generate star-grazers from bodies originating from the disk. However, this model does not seem to match all observational characteristics.

The purpose of this paper is to propose another mechanism involving mean-motion resonances with a single massive planet orbiting β Pic on a moderately eccentric ($e \gtrsim 0.05$) orbit as the main source of star-grazers. In Section 2, we describe all the dynamical constraints we can deduce from both observations and modeling, showing that these are strong enough to allow the distinction between different models, and we compare the proposed mechanisms to them. In Section 3, we develop our model, showing that the 3:1 and 4:1 mean-motion resonances are a very efficient potential source of star-grazers. We compare the results to the observational constraints. We also discuss the efficiency of the process as a function of the eccentricity of the planet's orbit and of its mass. In Section 4, we discuss the time-scales of the process and compare them to the age of the system. We show that a secular oscillation of the orbital eccentricity of the planet can considerably enlarge the basic time-scale of the mechanism, while keeping it active. Our conclusions are presented in Section 5.

2. THE DYNAMICAL PROBLEM

2.1. The Observational Constraints

Multiple observational campaigns, coupled with an intense modeling activity, have allowed us to deduce a small set of strong dynamical characteristics and/or constraints to the basic FEB scenario (Lagrange-Henri *et al.* 1992; Vidal-Madjar *et al.* 1994; Lagrange *et al.* 1995; Beust *et al.* 1995):

- The observed spectral features concern metallic ions coming from the evaporation of refractory elements. This requires high enough temperatures and it can be shown (Beust *et al.* 1995) that evaporation must take place closer than $\sim$35 R_* ($\simeq$0.25 AU), where R_* is the stellar radius. So, FEBs must have close approaches to the star.
- The simulations have indeed shown that some of the spectral events (mainly those most redshifted) must result from the evaporation of FEBs as close as 1 R_* or less to the stellar surface. However, it appears that a large variety of periastra in the FEB distribution (ranging between $\sim$2 R_* and $\sim$35 R_*) is needed to fit the observations.
- The relative lack of variation in the redshifted velocity of the spectral events, monitored in the Ca II, K and H lines, has been interpreted as an indication that the longitudes of the periastra of all FEBs must be almost aligned (Beust *et al.* 1990); as a matter of fact, a small dispersion of $\sim$10° around the mean value is needed (Beust *et al.* 1995).
- The evaporation rates, deduced from the magnitude of the detectable spectral features, correspond roughly to the total evaporation of a body of $\sim$1 km radius within a few days, i.e., in one periastron passage. Such a high evaporation activity is not surprising in the hot vicinity of β Pic (spectral type A5V, $T_{\rm eff} \simeq 8000$ K), but a major

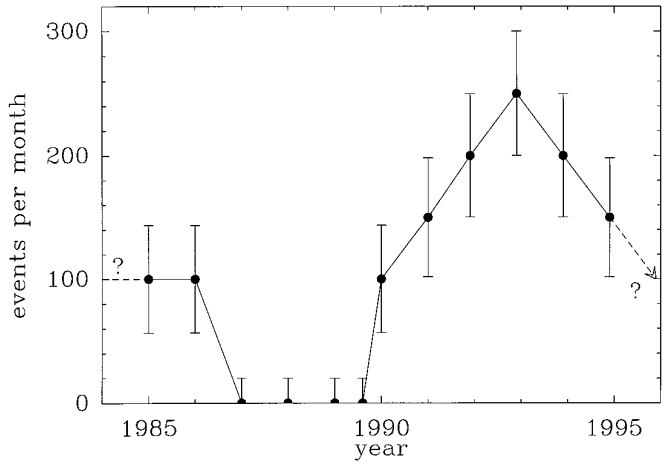

FIG. 1. Evolution of the frequency of FEB arrival near β Pic in the past years as roughly estimated from the survey of the activity in the Ca II, K and H lines.

consequence is that a FEB must be totally destroyed after a few passages through periastron. Therefore, the mechanism generating such an infall of bodies toward the star has to work on a more or less continuous basis.

• The flux rate of FEB infall can hardly be evaluated. It is certainly very high, but it changes on time-scales on the order of a year. In a period of highest activity (such as December 1992), it was estimated to be about one FEB every 3 hr. i.e., more than 200 FEBs per month (Beust *et al.* 1995). In contrast, the activity seemed to be very low at other epochs (nothing was detected during several days). A rough estimate of the evolution over the past 10 yr is displayed in Fig. 1. Note that this estimate has been derived from the survey of the visible Ca II, K and H lines toward β Pic at $\lambda = 3933.68$ and 3968.47 Å, respectively. The activity of other variable lines, e.g., Mg II, Al II, or Al III, mainly located in the UV part of the spectrum usually appeared well correlated with that general trend, although with some small differences. In particular, in 1987 the activity toward the Ca II lines appeared very low, while the activity toward the UV lines, surveyed with the IUE satellite, was significant (Lagrange-Henri *et al.* 1989). That peculiar observation might be of relevant interest for a dynamical model, since the events occurring in the UV lines, usually at the highest redshifted velocities, are precisely those related to the smallest periastron distances ($\sim$2–4 R_*), while the low-velocity events, occurring in the Ca II lines, are related to periastra ranging typically from $\sim$15 R_* to 35 R_* (Beust *et al.* 1990).

• The dispersion of the periastron distances q together with the high evaporation rates provide a very strong constraint: since some FEBs are observed with periastra as close as 1–3 R_*, and since a few periastron passages at less than $\sim$30 R_* are enough to completely destroy a FEB, we need quite a fast dynamical transport mechanism. Indeed, if the decrease of the periastron distance was slow with respect to the orbital period, then we could not observe FEBs at $q = 2R_*$: these objects, indeed, would have been completely destroyed before reaching $q = 2R_*$, passing several times at periastron with $2R_* < q < 30\ R_*$.

• The rate of the evaporated mass from the FEB scenario has been estimated to $\sim 2 \times 10^{-9}\ M_\oplus$ per year at most (Beust *et al.* 1995). This in itself is not a very strong constraint, because it depends on the duration of the phenomenon, which is unknown. The duration of the FEB phenomenon around β Pic must be long enough (at least 10^6–10^7 yr) to allow the present observation not to be too fortuitous. In any case, even assuming a duration of about 10^7 yr, the total mass evaporated from FEBs would be just on order of $10^{-2}\ M_\oplus$.

2.2. *Dynamical Mechanisms of Transport for FEBs*

Modern knowledge of the dynamics in the Solar System suggests several possible mechanisms for transporting bodies toward the central star. In the following we list the main mechanisms that we see at work in our Solar System, discussing their possible efficiency in the β Pic system and their agreement with the observational constraints.

(*I*) *The Kozai mechanism.* This mechanism is at work if there is at least one massive planet in the disk of β Pic and acts on objects with a small component,

$$\Theta = \sqrt{a(1 - e^2)} \cos i, \tag{1}$$

of the angular momentum vector on the direction which is orthogonal to the planetary orbital plane. Here a is the semimajor axis, e is the eccentricity, and i is the inclination of the small body's orbit with respect to the reference plane on which the planet orbits around the star. In particular, orbits with small eccentricity and large inclination evolve to small inclination and large eccentricity (Kozai 1962) with the precession of the argument of periastron ω. Along this motion, the semimajor axis is on the average constant and the periastron distance decreases. As pointed out by Bailey *et al.* (1992) (see also Thomas and Morbidelli 1995), this mechanism is responsible for the origin of most sungrazer comets in our Solar System, in particular those of the Kreutz group. Invoking this model for the transport of FEBs toward β Pic, however, gives rise to two major problems. On the one hand, one needs an important source of highly inclined orbits; the origin and the refilling of such a population of cometary bodies is difficult to explain on the basis of the models for the formation of the β Pic disk. On the other hand, corresponding to the minimal periastron distance, the argument of periastron ω assumes a well defined value, but the longitude of node Ω is not

constrained by the dynamics. In other words, there is a rotational invariance of the problem, so that one cannot explain the peculiar distribution of longitudes of periastra $\varpi = \omega + \Omega$ deduced from the analysis of the observations.

(*II*) *Hierarchical fragmentation of a large body.* This mechanism is suggested by the recent observations of comet Shoemaker–Levy 9: one single object is taken to a very elliptic orbit by some (even improbable) mechanism where it is broken by tidal forces. This gives origin to a group of comets with similar orbits. The Kreutz group of comets was also produced this way. This model explains well the large abundance of objects observed and the alignment of their periastra. However, it is difficult to explain in a straightforward way the large dispersion of periastron distances from 2 to 30 R_*, as deduced from the analysis of observations (Beust *et al.* 1995). Moreover, it is difficult to explain how the phenomenon of FEBs can last several years, with significant fluctuations of intensity with time.

(*III*) *Secular resonances.* Recently, it has been understood that the ν_6 secular resonance in the asteroid belt is strong enough to pump up the eccentricity of resonant orbits from 0 to 1 with the consequence of collision with the Sun (Farinella *et al.* 1994). We recall that the ν_6 secular resonance occurs where the frequency g of precession of the longitude of perihelion of the body is equal to the frequency g_6 of precession of the perihelion of Saturn. Recently, Levison *et al.* (1994) proposed this mechanism to be responsible for the FEB scenario in the β Pic system. This would indeed explain the alignment of periastra. However the extremely strong power of the ν_6 resonance in the asteroid belt is due to some specific aspects of our Solar System. Indeed, a resonance can be approximated by a pendulum-like Hamiltonian

$$H(p, q) = \frac{\alpha}{2} p^2 + \beta \cos q, \tag{2}$$

where p and q are canonically conjugated action-angle variables. The strength of the resonance is $4\sqrt{\beta/\alpha}$, which is the maximum variation amplitude of the action p along a resonant orbit. So, if α is small, the resulting resonance strength is very large. In the case of the ν_6 resonance, as pointed out first by Yoshikawa (1987), the local convexity α of the Hamiltonian is very small, since α becomes null at $a = 2.3$ AU for $i = e = 0$, i.e., in the region where the ν_6 resonance is approximately located. This is the reason why the ν_6 secular resonance is so strong. All other secular resonances indeed are much weaker. For example, the ν_5 resonance, which results from the corotation with the perihelion of Jupiter and which should be, in principle, stronger than the ν_6 resonance, can force the eccentricity to change only a few tenths (Morbidelli and Henrard 1991). So, we can conclude that the ν_6 mechanism is highly nongeneric and that it should not be expected to be at work in other planetary systems different from our Solar System. Indeed, if the planets had different masses or different mutual distances the power of the ν_6 resonance would be considerably reduced. As a matter of fact, in their paper, Levison *et al.* (1994) integrated fictitious bodies in the framework of our Solar System model, without even taking care about the fact that the mass of β Pic is approximately 1.5–2 times that of the Sun (Paresce 1991).

(*IV*) *Mean-motion resonances.* Mean-motion resonances are also known to pump up the eccentricity of resonant orbits up to Sun-grazing values (Moons and Morbidelli 1995; Morbidelli and Moons 1995). In the Solar System this is due to the overlapping of secular resonances inside the mean-motion resonances. However, a single planet on an elliptic orbit with eccentricity of about 0.1 would be able to pump the eccentricities of orbits in some mean-motion resonances up to 1, in particular the 4 : 1 and 3 : 1 resonances. This is our favorite model, and we expand it in the following sections. In our opinion it fits most of observational constraints; in particular it explains why the longitudes of periastra ϖ are aligned and why the flux of FEBs is modulated with time. Moreover, it is a very generic model: it is independent from the semimajor axis of the orbit of the planet and "mostly" independent of its mass also, so that it is likely to be at work in the formation of every planetary disk as well as in the β Pic disk. We stress finally that the existence of additional planets would only increase the efficiency of this transport mechanism of FEBs, probably activating other mean-motion resonances such as the 5 : 2.

3. MEAN-MOTION RESONANCES WITH A PLANET ON AN ECCENTRIC ORBIT AS A SOURCE FOR FEBS ONTO β PIC

We first recall briefly the basic elements of the dynamics in mean-motion resonances with a perturbing planet, i.e., in the frame of the elliptic planar restricted three-body problem. The Hamiltonian H_0 of the problem in a heliocentric reference frame can be written as usual (see, e.g., Henrard 1990, p. 238):

$$\frac{H_0}{GM} = -\frac{1-\mu}{2a} - \mu \left[\frac{1}{|\mathbf{r} - \mathbf{r}'|} - \frac{\mathbf{r} \cdot \mathbf{r}'}{r'^3} \right]. \tag{3}$$

Here M is the total mass of the system (star + planet), G is the gravitational constant, μ is the reduced mass of the planet (m(planet) = μM), and a is the semimajor axis of the test particle. Moreover, $\mathbf{r}$ and $\mathbf{r}'$ are the position vectors of the particle and of the planet, respectively, with respect

to the star. More generally, all primed quantities will hereafter refer to the planet and non-primed quantities to the particle.

This Hamiltonian is implicitly expressed as a function of the usual planar Delaunay elements of the particle:

$$\begin{aligned} \lambda &= \text{mean longitude}; & L &= \sqrt{(1-\mu)aGM} \\ \varpi &= \text{longitude of periastron}; & P &= L(\sqrt{1-e^2}-1). \end{aligned} \tag{4}$$

To take into account the $(p+q)$: p resonance, we perform the following canonical transformation:

$$\begin{aligned} \sigma &= \frac{p+q}{q}\lambda' - \frac{p}{q}\lambda - \varpi; & \Sigma &= -\frac{q}{p}L \\ \nu &= \varpi - \varpi'; & N &= L\left(\sqrt{1-e^2} - \frac{p+q}{p}\right). \end{aligned} \tag{5}$$

The variable σ is usually called the "critical angle of resonance" (Moons and Morbidelli 1995). Since the above transformation is time-dependent through λ' (which is assumed to be a given linear function of time), the Hamiltonian in the new variables becomes

$$H = H_0 - \frac{p+q}{p}n'L, \tag{6}$$

where n' is the mean motion of the planet. The Hamiltonian is then averaged over the only remaining fast variable, i.e., λ'. This transforms the time-dependent Hamiltonian into a time independent (conservative) one.

In the case where the orbit of the perturbing planet is circular (circular restricted planar three-body problem), the Hamiltonian obviously does not depend on ν, since ϖ' is undefined. This may be verified directly from Eq. (3). The quantity N is therefore conserved. This can be rewritten as

$$N = \sqrt{a}\left(\frac{p+q}{p} - \sqrt{1-e^2}\right) = \text{cst}. \tag{7}$$

The resonant region is defined as the portion of the a, e space where σ librates. Resonant regions have a typical V-shaped form as one can see in Figs. 2 and 3. The amplitude of the resonant regions scales as the square root of the reduced mass μ of the perturbing planet with respect to the central star. In Figs. 2 and 3 we show the border of the 4:1 and 3:1 resonances, respectively, computed for μ equal to 5×10^{-4}, 1×10^{-3}, and 5×10^{-3}. The semimajor axis is expressed in relative units, where a' (the semimajor axis of the planet) is 1. Indeed, the problem simply rescales with a'.

The effect of a mean-motion resonance is to force the oscillation of the semimajor axis a of the resonant body, coupled with the libration of σ. The maximal amplitude of oscillation of a is bound by the borders of the resonant region. Due to Eq. (7), the oscillation of a is coupled to the oscillation of the eccentricity e, but the latter is in general of small amplitude.

When the perturbing planet is on an eccentric orbit the Hamiltonian (6) depends on ν, so that the quantity N is no longer conserved. Therefore, the eccentricity changes, forced by the motion of $\nu = \varpi - \varpi'$, over a time scale which is much longer than the one concerning the oscillation of a and σ; moreover, as a consequence of adiabatic invari-

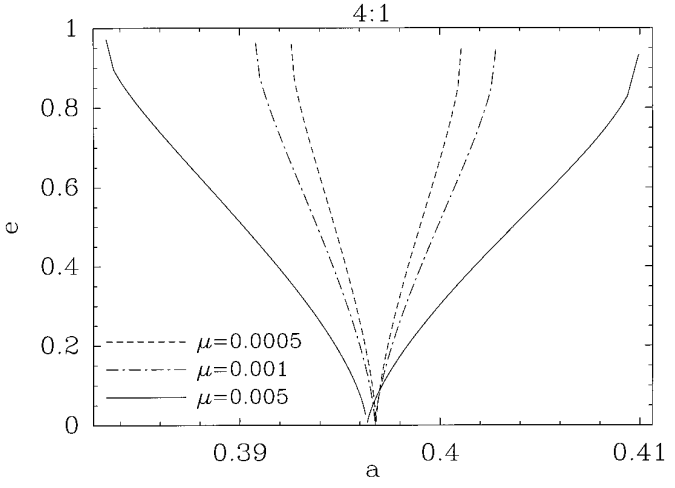

FIG. 2. Resonant regions in (a, e) space for the 4:1 resonance, for three different values of μ. The resonant region lies inside the V-shaped curve. The width of the resonant region is clearly an increasing function of μ. The slight displacement of the bottom of the curve from one value to each other is also due to the variation of μ, because the "exact resonance value" a_0 for the semimajor axis scales as $(1-\mu)^{1/3}$.

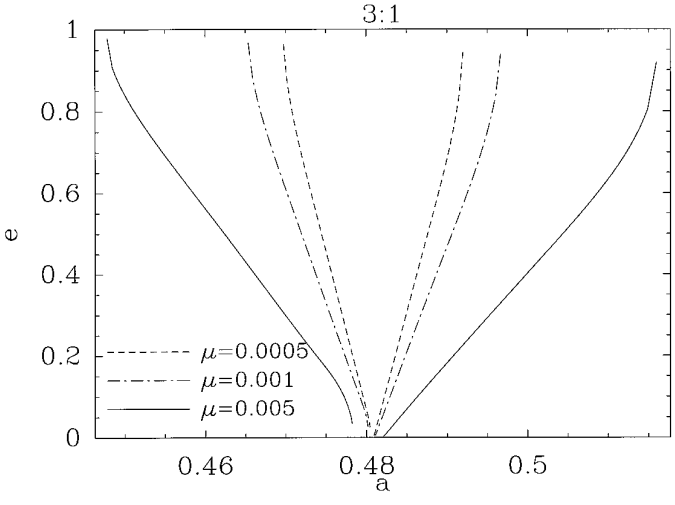

FIG. 3. Same as Fig. 2, but for the 3:1 resonance. Note the nonzero width of the resonant region at $e = 0$.

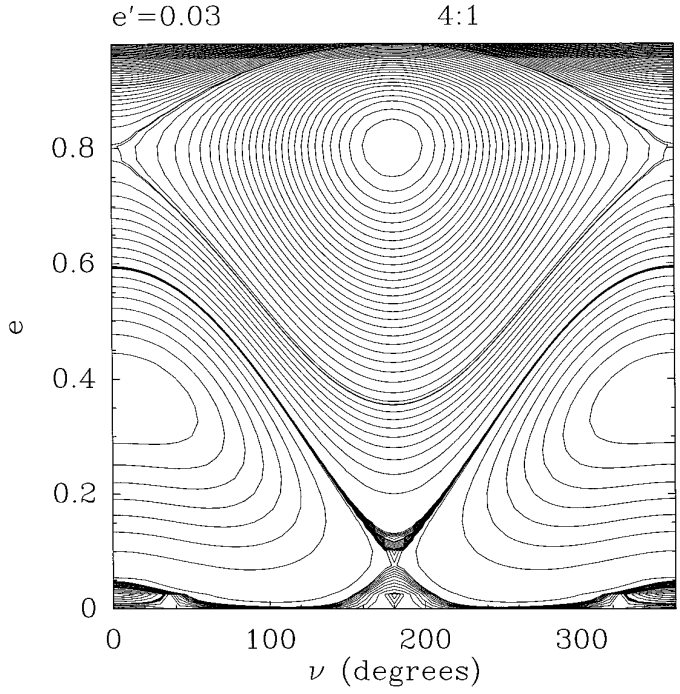

FIG. 4. Level curves of the Hamiltonian in a ($\nu = \varpi - \varpi'$, e) plane, for the 4:1 resonance case and for an eccentricity of the perturbing planet $e' = 0.03$. The values of a and σ have been fixed to those corresponding to the exact resonance.

ance, the amplitude of oscillation of a is roughly conserved along the secular changes of e. Yoshikawa (1989) computed the secular changes of e in most mean-motion resonances with Jupiter in our Solar System. He found that these changes are particularly relevant for the 4:1, 3:1, and 5:2 resonances. His computations have been made assuming $e' = 0.048$ and taking into account that ϖ' precesses with a frequency equal to 4.207 arc sec/yr. However, it is evident from the structure of the equations of motion that the results are very sensitive to the value of e'. Therefore, in the following we will explore the secular dynamics inside the 4:1, 3:1, and 5:2 resonances for different values of e' in order to find out if a planet with a sufficiently large eccentricity e' would be able to pump the eccentricity of resonant bodies up to 1, giving origin to FEBs onto the central star. Since our description of the secular dynamics must be correct for all eccentricities ranging from 0 to 1, we will not use the classical expansions of the equations of motion in powers of e, typical of celestial mechanics. The Hamiltonian of the problem will be evaluated numerically at any point a, e, σ, $\varpi - \varpi'$ as explained in Moons (1994).

Conversely, the dynamics is not very sensitive to the value of the planetary mass, i.e., the parameter μ. The analysis detailed below assumed $\mu = 0.001$, but taking $\mu = 0.005$ or $\mu = 5 \times 10^{-4}$ gives almost the same curves as presented below. With a stellar mass of 1.5–2 $M_\odot$, $\mu = 0.001$ corresponds to a planet 1.5–2 times as massive as Jupiter. This just means that we consider that if several planets are present in the β Pic disk, the dynamics of small bodies in that system is mostly constrained by the most massive one, which should be expected to be a giant planet.

We start our analysis from the 4:1 resonance and we focus on resonant orbits with small amplitude of libration of a. The secular dynamics can be represented on the plane ($\varpi - \varpi'$, e), the curves denoting the evolution of e with the circulation or libration of $\nu = \varpi - \varpi'$. Figures 4, 5, and 6 refer to the cases $e' = 0.03$, $e' = 0.05$, and $e' = 0.1$, respectively, and ϖ' is assumed to be fixed in all cases.

In the first case ($e' = 0.03$), the 4:1 resonance cannot be a source for FEBs toward β Pic. Indeed, considering particles on originally quasi-circular orbits, we note that the eccentricity is pumped only up to 0.6, by the libration of ν around 0. This is not enough to have close approaches to the central star within a few stellar radii. The region where ν circulates is also unable to pump the eccentricity up enough to generate FEBs. We also notice a second island of libration of ν around 180°, which can indeed pump the eccentricity up to 1, but only for orbits having already a quite large eccentricity.

When $e' = 0.05$ (Fig. 5), the situation is drastically different. Now, the island of libration around $\nu = 0$ does not extend down to $e = 0$. Conversely, the island of libration

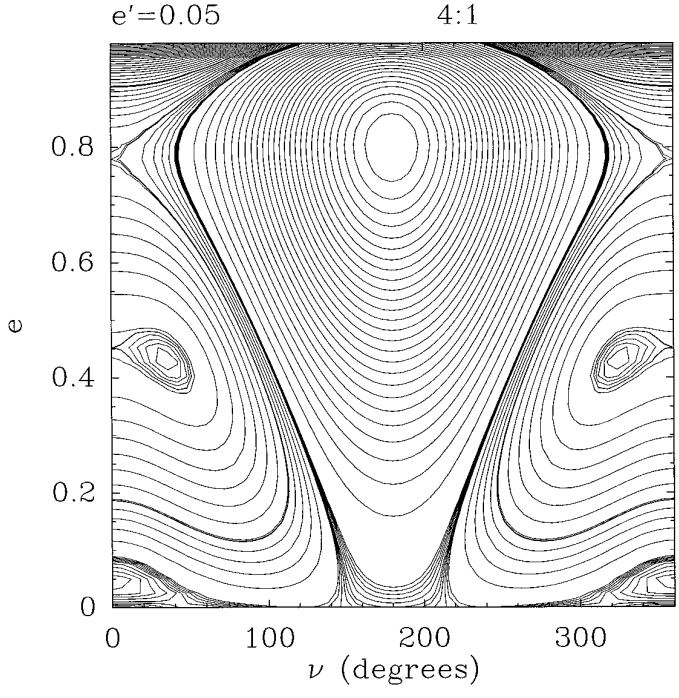

FIG. 5. Same as Fig. 4, still for the 4:1 resonance case but for $e' = 0.05$.

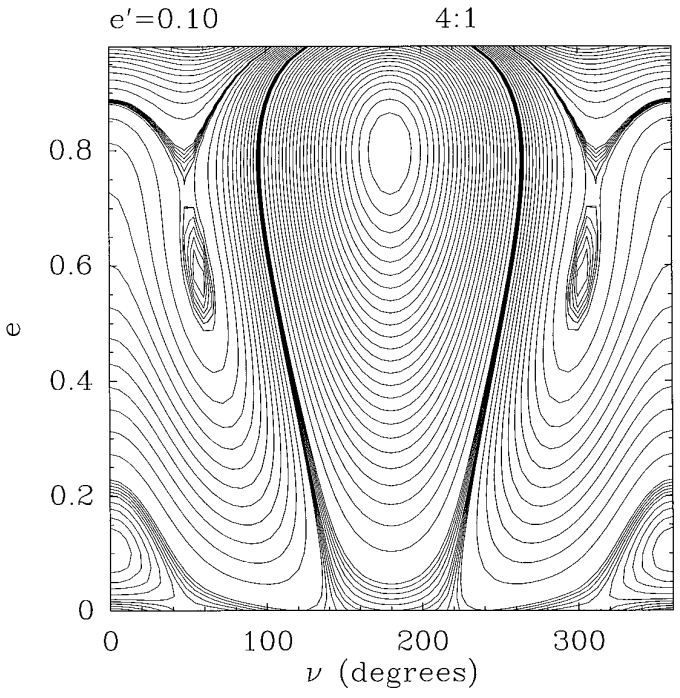

FIG. 6. Same as Fig. 4, but for $e' = 0.1$.

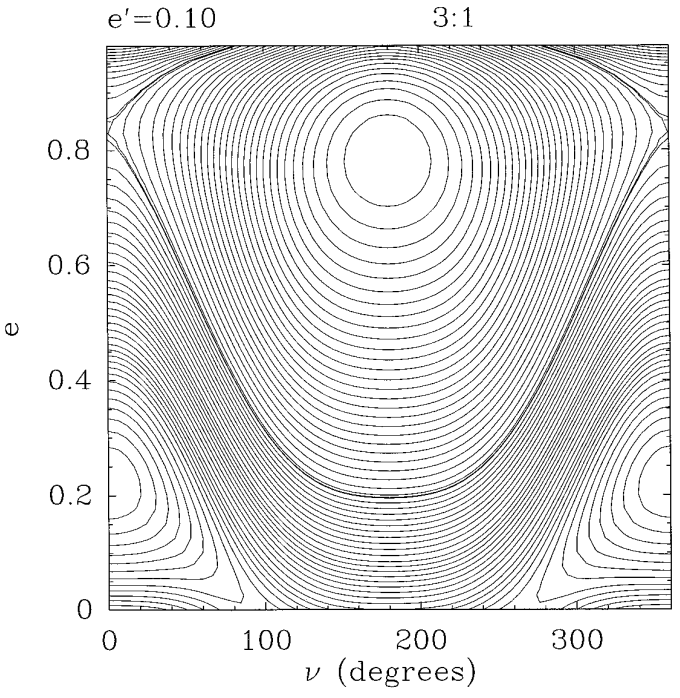

FIG. 8. Same as Fig. 7, but for $e' = 0.1$.

around $\nu = 180°$ does, so that the eccentricity of almost circular orbits is pumped up to 1, originating the FEB phenomenon.

When $e' = 0.1$ (Fig. 6), the islands of libration around $\nu = 0$ almost disappears; as a consequence, almost all orbits, even those with initial $e \sim 0$, are forced to evolve to $e = 1$. In this case, as in the previous one, we can therefore conclude that the 4:1 resonance could be an active source for FEBs. We remark moreover that the final values of the longitude of periastron $\varpi - \varpi'$ at $e = 1$ would be confined between 100° and 140° for all orbits with initial eccentricities below 0.3. Note that the symmetric interval 220–260° is excluded because the Hamiltonian dynamics fixes the exploration direction of the curves. In the present case, the closed curves in Figs. 4 are explored clockwise. Consequently, the 220–260° interval for ϖ would correspond to bodies with a decreasing eccentricity, after their closest stellar approach. Since the FEBs are expected to be completely destroyed after a few close periastron passages (Beust *et al.* 1995), we do not expect to detect them in that part of the (ν, e) diagram.

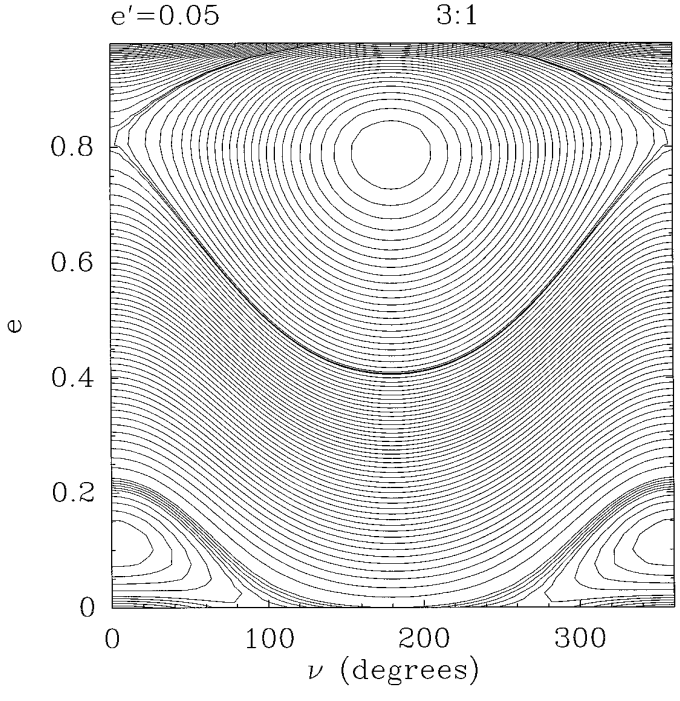

FIG. 7. Same as Fig. 4, but for the 3:1 resonance case and for $e' = 0.05$.

Assuming different values for the reduced mass μ of the planet does not change the picture of the secular dynamics. However, acting on the amplitude of the mean-motion resonance, μ determines the volume of the phase space affected by the mechanism of eccentricity-pumping, as illustrated in Figs. 5 and 6.

Figures 7 and 8 refer to the case of the 3:1 resonance. If $e' = 0.05$ (Fig. 7) the island of libration of ν around 0 pumps the eccentricity only up to 0.2. The large island of libration around $\nu = 180°$ brings to 1 only orbits with large initial eccentricity ($\gtrsim 0.45$). Conversely, in the case $e' = 0.1$ (Fig. 8) this latter island becomes much larger. In this case, orbits with initial $e \gtrsim 0.2$ at $\nu = 180°$ are forced to

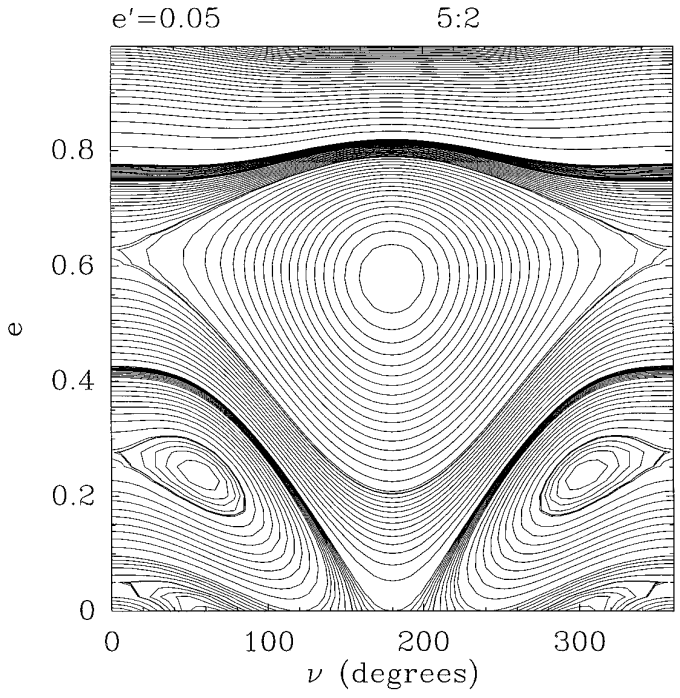

FIG. 9. Same as Fig. 4, but for the 5:2 resonance case and $e' = 0.05$.

increase their eccentricity to 1. If we assume that on the β Pic disk the average and the dispersion of the eccentricities of the bodies are equivalent to those typical of the asteroid belt, then also the 3:1 resonance could be an active source of FEBs on β Pic. We remark that the periastra ϖ of FEB's orbits with initial eccentricities between 0.2 and 0.3 would be confined between 80° and 120° from the planet's periastron ϖ'. Again, the symmetric interval 240°–280° is excluded because of the direction of the dynamics, as in the 4:1 case.

Finally, in Figs. 9 and 10 we consider the case of the 5:2 resonance. It is immediately evident that both in the case $e' = 0.05$ and $e' = 0.1$ the eccentricity of a resonant orbit is pumped up a lot, but cannot reach the value $e = 1$. Therefore the 5:2 resonance *cannot* be a source of FEBs, at least in the framework of this simple one-planet model.

All other mean-motion resonances produce smaller effects on the secular evolution of the eccentricity than the 4:1, 3:1, and 5:2 ones, according to Yoshikawa's paper (1989), so that they are not likely to be the source of FEBs even in the case $e' = 0.1$. The 7:3 and 2:1 mean-motion resonances also cause substantial eccentricity increases, but like the 5:2 resonance, they never make bodies evolve to star-grazing orbits. Therefore, we can conclude that the 4:1 and 3:1 resonances should be the main active sources for FEBs in the β Pic disk.

We stress that the mean-motion resonance model fits very well two observational constraints. The first is the alignment of longitude of periastra of FEBS; the second concerns the modulation of the flux rate of FEBs with time.

The confinement of ϖ at large eccentricities is highlighted in Fig. 11. This figure is the same as Fig. 5 ($e' = 0.05$), but we use the periastron $Q = a(1 - e)$ in logarithmic scale as ordinate instead of e. This causes an enlargment of the high eccentricity region of Fig. 5. Assuming $a' = 10$ AU (which is just considered as a typical possible value), various stellar distances are indicated, delimiting the region of FEB evaporation. Together with the time-scale of the whole process, which is based on the value of the planetary revolution, this is the only point where the model depends on the planetary semimajor axis a'. We see that this dependence is very weak, since multiplying or dividing a' by a small factor does not affect the conclusion presented below.

The two bold curves on Fig. 11 also delimit the region of FEB evaporation. The upper curve separates FEBs that could evolve from low to high eccentricity from hypothetical bodies which would permanently remain at high eccentricity. The lower curve corresponds to the closed curve on Fig. 5 which has a minimum eccentricity $e = 0.05$ for $\nu = 180°$. Therefore, only the FEBs moving between the two bold curves may indeed evolve from a circular orbit to star-grazing orbits. Moreover, the observational constraint $\varpi = \text{cst} \pm 10°$ was deduced from repeated observations of variable low-velocity Ca II lines (Beust *et al.* 1995); these peculiar features are interpreted as resulting from

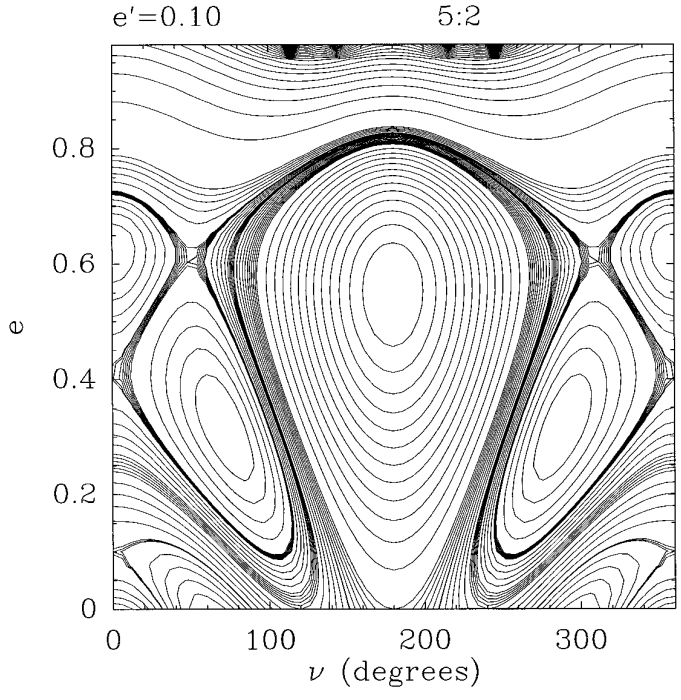

FIG. 10. Same as Fig. 9, but for $e' = 0.05$.

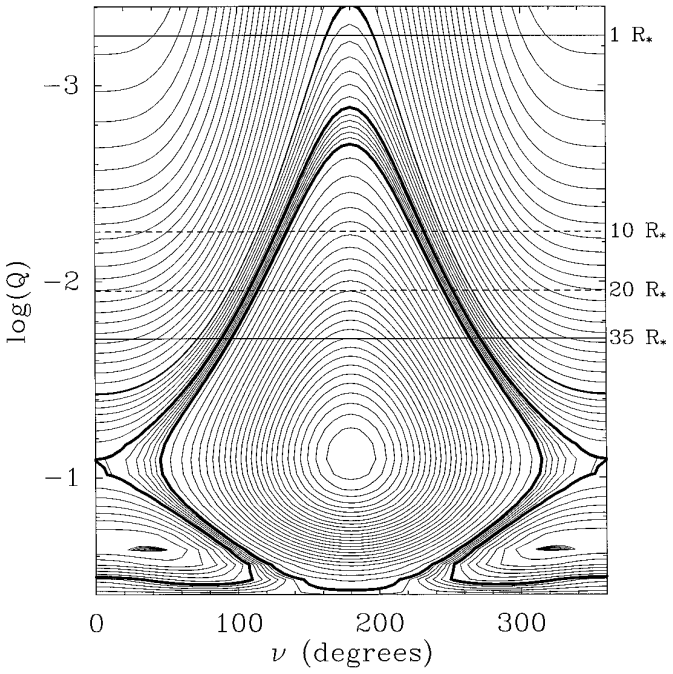

FIG. 11. Diagram equivalent to Fig. 5, but using the periastron $Q = a(1 - e)$ (normalized by the planetary semimajor axis) as ordinate in logarithmic scale, instead of e. The horizontal solid lines correspond to the stellar surface ($1\ R_*$), assuming a value of 10 AU for the planetary semimajor axis, and $R_* = 1.2\ R_\odot$. Other stellar distances values are indicted by dashed lines. The two bold curves delimit the region of the diagram where the FEBs are suppose to evolve.

bodies having periastra located between $\sim 10\ R_*$ and the $35\ R_*$ limit. FEBs with closer approaches generate high velocity events, mostly in the UV lines, for which ϖ is observationally far less constrained (Beust *et al.* 1990). The "ϖ-confinement" region for FEBs appears thus on Fig. 11 as a narrow band for which $\varpi = 110 \pm 20°$, i.e., close to the observational constraint. Note that this constraint was only roughly determined, so that a $\pm 15°$ or even $\pm 20°$ uncertainty for ϖ would also fit the data. Note finally that the ϖ confinement is much stronger for larger values of e', such as 0.1 (Fig. 5).

If the confinement condition for ϖ is satisfied also in the model by Levison *et al.* (1994), the second observational constraint, i.e., the modulation of the flux rate of FEBs with time, cannot be explained on the basis of the ν_6 resonance model. Conversely, if the FEBs originate from mean-motion resonances, they must have values of σ (the critical angle of the mean-motion resonance) confined around the exact resonant values ($\sigma = 0°, 120°, 240°$ for the 4:1 resonance and $\sigma = 90°, 270°$ for the 3:1 resonance). From the definition of σ above, and recalling that ϖ must be around 110° to satisfy the condition $e \simeq 1$, the mean longitude λ of FEBs is related to the planet's mean longitude λ'. Therefore, FEBs must pass through periastron (i.e., $\lambda = \varpi$) only at some specific dates. As shown in Section 2.1, the flux rate of FEBs onto β Pic seems to present large fluctuations over a timescale of about 7 yr (Fig. 1). Unfortunately, the timespan over which observations are available is too short to detect the periodicity in the flux rate of FEBs that the mean-motion resonance model predicts; however, over the next decade this will hopefully be possible. If the 4:1 resonance is the only active source, then we expect the flux rate of FEBs to fluctuate sinusoidally with time; if the 3:1 resonance is an active secondary source, then the infall rate should still be periodic, but is expected to present a more complex temporal dependance. We stress that if the flux rate of FEBs is confirmed to be periodic and can be separated into two components with relative period 3:4, then

(a) we will have the final proof that FEBs come from 3:1 and 4:1 resonances and could measure the relative efficiency of the two sources;

(b) we will determine the semimajor axis of the orbit of the perturbing planet and its mean longitude λ', i.e., its position in the β Pic disk. This would be of invaluable importance for future campaigns of direct observations of a planet around β Pic.

The present analysis does not provide any relevant constraint for the semimajor axis of the planet a', nor for its mass. This is not surprising, since the model depends only weakly on these parameters. The mass of the planet should affect the amount of small bodies evolving to star-grazers, since the width of the resonant region depends on μ (Figs. 2 and 3). However, it also depends on the amount of potential bodies available in the disk, and in particular in the resonant regions. This last parameter is not known, so it is impossible to put any constraint on the mass of the planet that way. Nevertheless, as we think that the dynamics of small bodies in the β Pic disk should be dominated by the most massive planet, we may suggest that our hypothetical planet is a gaseous giant rather than a terrestrial planet.

As a final remark, we point out that our model does not exclude the presence of several planets in the β Pic disk. In order not to reduce the efficiency of the 4:1 and 3:1 mean-motion resonances, we have to assume that there are no massive inner planets. Otherwise close encounters with the inner planets could take the bodies away from the mean-motion resonances before their eccentricity reaches star-grazing values. Conversely, the existence of several outer planets would even increase the efficiency of mean-motion resonances in transporting FEBs. First of all, the existence of several planets allows us to justify the fact that the eccentricity of the resonant perturbing planet e' can be (at least temporarily) on the order of 0.05 or even 0.1. Second, the additional perturbations provided by the outer planets increase the number of degrees of freedom

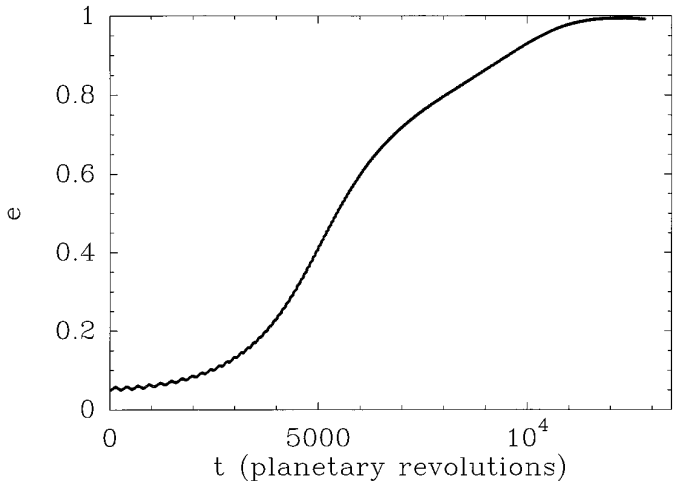

FIG. 12. Evolution versus time of the eccentricity of a test particle trapped in a 4:1 resonance with a perturbing planet of eccentricity $e' = 0.05$, as numerically integrated with the Extended Schubart Integrator. The particle, with initial eccentricity $e = 0.05$, falls onto the star after ~12,000 planetary revolutions.

in the secular problem, which then turns out to be no longer integrable. For example, the gap between the two islands of libration of ν existing in the 4:1 resonance in the case $e' = 0.03$ (Fig. 4) could be crossed, allowing the transport of FEBs toward β Pic even if e' is only 0.03. Also in the 5:2 resonance objects could reach $e = 1$ if the regular region at large e is destroyed. As a matter of fact, in our Solar System both the 3:1 and the 5:2 resonances can pump any resonant body up to $e = 1$ even if its initial eccentricity close to 0. It is important to stress that the mechanism we are pointing out here is quite generic. We do not need two ad hoc planets as in the model by Levison *et al.* (1994); we just need a major planet with a somewhat moderate eccentricity e', and eventually some noise due to the presence of additional outer planets. It is very likely that such a system could exist in the β Pic disk.

4. TIME-SCALES PROBLEMS CONNECTED TO THE ORIGIN OF FEBS ON β PIC

Now we discuss the time-scales of the transport process of FEBs to $e \simeq 1$ in mean-motion resonances. To test the efficiency of the mechanism suggested by the analysis of Section 3 numerically, we carried out numerical integrations of the motion of resonant test particles. The computations were done using the Extended Schubart Integrator (Moons 1994). This code integrates numerically the averaged equations of motion, deduced from the Hamiltonian (6).

Figures 12 and 13 show the evolution of the eccentricity vs time in the 4:1 resonance case with $e' = 0.05$ and in the 3:1 resonance case with $e' = 0.1$. The advantage of the Extended Schubart Integrator, compared to the theoretical pictures in Figs. 4–10, is that one is not limited here to small amplitudes of libration of a inside the mean-motion resonance, and it is not necessary to assume that such a small amplitude is conserved adiabatically with the secular change of the eccentricity. Moreover, one is not constrained by a *planar* model, and the inclination can be assumed to be different from 0. In any case the agreement between the results given by the Extended Schubart Integrator and the global theoretical pictures is excellent.

As one sees, a body becomes a star-grazer about about 12,000 planetary revolutions in the 4:1 resonance, and after only 2500 planetary revolutions in the 3:1 case. This time-scale shortens with increasing planetary eccentricity e'. Note also that the initial eccentricity of the small body is quite large ($e = 0.2$) in Fig. 13, whereas it is much smaller ($e = 0.05$) in Fig. 12. This is in agreement with the behavior deduced from Figs. 5 and 8. Indeed, taking a smaller initial eccentricity in the 3:1 resonance case does not generate any star-grazer. Concerning the inclination (not plotted here), starting with moderate values ($i \sim 1°$) it shows significative oscillations only when the eccentricity becomes larger than 0.6. However in the cases of Fig. 12 and Fig. 13 (as in most of all the cases that we have studied) it never exceeds 15°, a value which is still compatible with the observational constraints deduced from linedepth comparisons in the frame of the FEB scenario (Lagrange *et al.* 1995).

A time-scale of a few thousand planetary revolutions is, at the same time, both too long and too short. It is too long to explain why FEBs are "observed" to pass at a

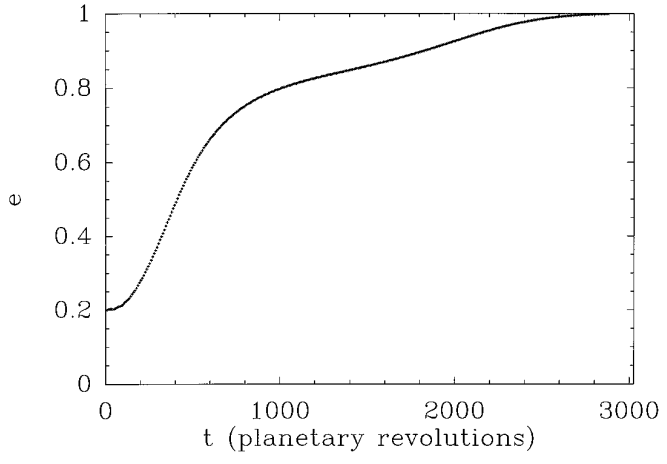

FIG. 13. Same as Fig. 12, but for a test particle trapped in a 3:1 resonance with the planet and $e' = 0.1$. The body falls onto the star after only ~2500 planetary revolutions, but one must note that the initial eccentricity is quite large ($e = 0.2$).

distance to β Pic ranging from 2 to 30 stellar radii. Indeed, if the eccentricity increases so slowly, then a FEB would decrease the periastron distance q of less than 1 R_* per revolution. Therefore, it is very difficult to explain how we can observe FEBs at a few R_* from β Pic, since these objects should already have been completely evaporated during the previous passages close to the star. This problem exists as well in all other models for the transport of FEBs to β Pic, such as those invoking the ν_6 secular resonance (an even slower process) or the Kozai mechanism. One needs eccentricity changes of a few percentages over one orbital period in order to explain how an object can pass at 2 R_* without making several revolutions at periastron $q < 30\,R_*$, which would completely destroy it. The dynamics in the restricted three-body problem does not provide any justification for these changes. In our opinion, the most reasonable model is to assume that close encounters of FEBs with planetesimals in the β Pic disk (which must exist in large numbers) add some noise to the secular evolution of the eccentricity allowing random changes of a few percentages over one revolution.

On the other hand, a time-scale of a few thousand planetary revolutions is too short to explain why the 4:1 and 3:1 resonances in the β Pic disk are not completely void of objects today, namely ~100 myr after the formation of the system. Why can we still observe FEBs? We have two possible answers to this problem. First, mean-motion resonances could be refilled continuously. This could be due to the fact that the location of mean-motion resonances shifts with time, since the resonant planet changes its own semimajor axis by ejecting planetesima on hyperbolic orbits. New objects are therefore captured into the mean-motion resonances. A second possibility is that the eccentricity of the resonant planet e' changes with time due to the presence of additional outer planets, so that the value $e' \gtrsim 0.05$ or $e' \sim 0.1$ is reached only temporarily. As a consequence, FEBs could reach the limit $e = 1$ only when e' is large, and this could increase the time-scale for the depletion of all objects in mean-motion resonances by several orders of magnitude. In order to better illustrate this possible phenomenon, at least from the qualitative point of view, we modified the Extended Schubart Integrator, assuming that the planet's eccentricity e' changes from 0 to 0.1 in a harmonic fashion over a period of about 30,000 planetary revolutions. The secular evolution of the eccentricity of an object in the 4:1 mean-motion resonance is given in Fig. 14. One sees that the eccentricity remains moderate for a long time and then suddenly increases to star-grazing values. The time-scale then is 2×10^5 planetary revolutions, much longer than the typical time-scale of the system where e' is permanently equal to 0.05 (Fig. 12). Then, it seems realistic that the 4:1 and 3:1 mean-motion resonances have not been yet completely depleted of objects and that one can still observe the FEB phenomenon.

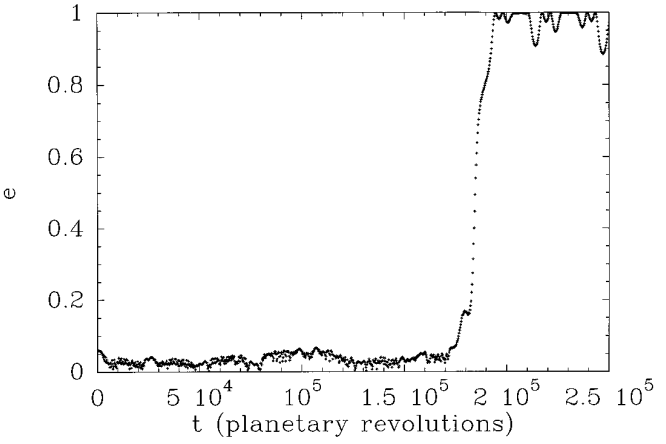

FIG. 14. Evolution versus time of the eccentricity of a test particle trapped in a 4:1 resonance with a perturbing planet whose eccentricity is sinusoidally time-variable over a period of 30,000 revolutions, as integrated with the Extended Schubart Integrator. The particle falls onto the star after ~200,000 planetary revolutions.

5. CONCLUSIONS

In this paper we have shown that the idea of the existence of falling evaporating bodies onto β Pic, first invoked in order to explain some spectral anomalies of the star, is realistic from a dynamical point of view. Our favorite model is that FEBs come from the 4:1 and the 3:1 mean-motion resonances with a major planet, the eccentricity of which is (at least temporarily) on the order of 0.05 or more. This model explains why the longitude of periastra of the orbits of FEBs are aligned within quite a small interval of values. Moreover, it explains why the observed flux rate of FEBs into β Pic changes strongly with time. We point out that if in the future a periodicity of the flux rate of FEBs is detected, one will have the observational proof that these objects come from mean-motion resonances. Then we will be able to measure the comparative efficiency of the different resonances and will be able to determine the orbit and the position of the planet the β Pic disk.

The fact that FEBs are observed today, namely $\lesssim$100 myr after the formation of the β Pic system, is quite a strong constraint: it implies that mean-motion resonances must not be completely depleted of objects yet. This can be explained assuming that resonance locations shift with time due to a secular drift of the planet's orbit caused by hyperbolic ejection of bodies; in this way, resonances would capture continuously new bodies, which then will become FEBs after the eccentricity of their orbit has been sufficiently increased. A second possibility is that the eccentricity of the perturbing planet changes with time, due to the presence of additional outer planets. In this way, the condition $e' \gtrsim 0.05$ would be fulfilled only temporarily,

which would easily increase the time-scales of the transport phenomenon of transport of FEBs up to millions of years.

Finally, the fact that the periastron distance of FEBs from β Pic ranges from 2 to 35 stellar radii, makes us assume that frequent close encounters between FEBs and other small bodies in the β Pic disk must occur, in order to explain fast changes of the eccentricity of a few percentages during one revolution. Conversely, bodies with a mass comparable to that of big terrestrial planets should be absent; otherwise the FEB-candidates would be ejected from mean-motion resonances before becoming star-grazing.

REFERENCES

Aumann, H. H., F. C. Gillett, C. A. Beichman, T. de Jong, T., J. R. Houck, F. J. Low, G. Neugebauer, R. G. Walker, and P. R. Wesselius 1984. Discovery of a shell around α Lyr. *Astrophys. J.* **278,** L23–L27.

Bailey, M. E., J. E. Chambers, and G. Hahn 1992. Origin of star-grazers: A frequent cometary end-state. *Astron. Astrophys.* **257,** 315–322.

Beust, H., A. M. Lagrange-Henri, A. Vidal-Madjar, and R. Ferlet 1990. The β Pictoris circumstellar disk. X. Numerical simulations of infalling evaporating bodies. *Astron. Astrophys.* **236,** 202–216.

Beust, H., and J. J. Lissauer 1994. The effects of stellar rotation on the absorption spectra of comets orbiting β Pictoris. *Astron. Astrophys.* **282,** 804–810.

Beust, H., and M. Tagger 1993. A hydrodynamical model for infalling evaporating bodies in the β Pictoris circumstellar disk. *Icarus* **106,** 42–58.

Beust, H., A. Vidal-Madjar, and R. Ferlet 1991. The β Pictoris protoplanetary system. XII. Planetary perturbations in the disk and star-grazing bodies. *Astron. Astrophys.* **247,** 505–515.

Beust, H., A.-M. Lagrange, F. Plazy, and D. Mouillet 1996. The β Pictoris circumstellar disk. XXII. Investigating the model of multiple cometary infalls. *Astron. Astrophys.*, in press.

Boggess, A., F. C. Bruhweiler, C. A. Grady, D. C. Ebbets, Y. Kondo, L. M. Trafton, J. C. Brandt, and S. R. Heap 1991. First results from the Goddard high-resolution spectrograph: Resolved velocity and density structures in the β Pictoris circumstellar disk. *Astrophys. J.* **377,** L49–L52.

Bruhweiler, F. C., Y. Kondo, and C.A. Grady 1991. Mass outflow in the nearby proto-planetary system. β Pictoris. *Astrophys. J.* **371,** L27–L31.

Farinella, P., Ch. Froeschilé, C. Froeschlé, R. Gonczi, G. Hahn, A. Morbidelli, and G. B. Valsecchi 1994. Asteroids falling onto the Sun. *Nature* **371,** 315–317.

Golimowski, D. A., S. T. Durrance, and M. Clampin 1993. Coronographic imaging of the β Pictoris circumstellar disk: Evidence of changing disk structure within 100 AU. *Astrophys. J.* **411,** L41–L44.

Gor'kavyi, N. N., and T. A. Taidakova 1995. β Pic and numerical study of the giant planet hypothesis. In *Circumstellar Dust Disk and Planet Formation* (*10th IAP meeting*) (R, Ferlet and A. Vidal-Madjar, Eds.), pp. 99–104. Editions Frontières.

Grady, C. A., F. C. Bruhweiler, K.-P. Cheng, W. A. Chu, and Y. Kondo 1991. The circumstellar disks of β Pictoris analogs. *Astrophys. J.* **367,** 296–301.

Henrard, J. 1990. Action-angle variables—semi-numerical perturbations method. In *Modern Methods in Celestial Mechanics, Goutelas 1989* (D, Benest and C. Froeschlé, Eds.), pp. 213–248. Editions Frontières.

Hobbs, L. M., A, Vidal-Madjar, R. Ferlet, C, E, Albert, and C. Gry 1985. The gaseous component of the disk around β Pictoris. *Astrophys. J.* **293,** L29–L33.

Kondo, Y., and F. C. Bruhweiler 1985. IUE observations of β Pictoris: An IRAS candidate for a protoplanetary system. *Astrophys. J.* **291,** L1–L5.

Kozai, Y. 1962. Secular perturbations of asteroids with high inclination and eccentricities. *Astron. J.* **67,** 591–598.

Lagage, P.-O., and E. Pantin 1994. Dust depletion in the inner disk of Beta Pictoris as a possible indicator of planets. *Nature* **369,** 628–630.

Lagrange-Henri, A.-M., H. Beust, A., Vidal-Madjar, and R. Ferlet 1989. The β Pictoris circumstellar disk. VIII. Evidence for a clumpy structure of the infalling gas. *Astron. Astrophys.* **215,** L5–L8.

Lagrange-Henri, A.-M., E. Gosset, H. Beust, H., R. Ferlet, and A, Vidal-Madjar 1992. The β Pictoris circumstellar disk. XIII. Survey of the variable Ca II lines. *Astron. Astrophys.* **264,** 637–653.

Lagrange, A.-M., F. Plazy, H. Beust, D. Mouillet, M. Deleuil, R. Ferlet, J. Spyromilio, A. Vidal-Madjar, W. Tobin, J. B. Hearnshaw, M. Clark, and K. W. Thomas 1996. The β Pictoris circumstellar disk. XXI. Results of the December 1992 spectroscopic campaign. *Astron. Astrophys.*, in press.

Lazzaro, D., B. Sicardy, F. Roques, and R. Greenberg 1994. Is there a planet around β Pictoris? Perturbations of a planet on a circumstellar dust disk. 2. The analytical model. *Icarus* **108,** 59–80.

Lecavelier des Etangs, A., G. Perrin, R. Ferlet, A. Vidal-Madjar, F. Colas, C. Buil, F. Sèvre, J.-E. Arlot, H. Beust, A,-M. Lagrange-Henri, J. Lecacheux, M. Deleuil, and C. Gry 1993. Observations of the central part of the β Pictoris disk with an anti-blooming CCD. *Astron. Astrophys.* **274,** 877–882.

Levison, H. F., M. J. Duncan, and G. W. Wetherill 1994. Secular resonances and cometary orbits in the β Pictoris system. *Nature* **372,** 441–444.

Lissauer, J. J. 1993. Planet formation. *Annu. Rev. Astron. Astrophys.* **31,** 129–174.

Moons, M. 1994. Extended Schubart integrator. *Celest. Mech. Dynam. Astron.* **60,** 173–186.

Moons, M., and A. Morbidelli 1995. Secular resonances inside mean motion commensurabilities: the 4/1, 3/1, 5/2, and 7/3 cases. *Icarus* **114,** 33–44.

Morbidelli, A., and J. Henrard 1991. The main secular resonances ν_6, ν_5 and ν_{16} in the asteroid belt. *Celest. Mech. Dynam. Astron.* **51,** 169–197.

Morbidelli, A., and M. Moons 1995. Numerical evidences on the chaotic nature of the 3/1 resonance. *Icarus* **115,** 60–65.

Mouillet, D., and A.-M. Lagrange 1995. The β Pictoris circumstellar disk XX. Some physical parameters of the gaseous component. *Astron. Astrophys.* **297,** 175–182.

Paresce, F. 1991. On the evolutionary status of β Pictoris. *Astron. Astrophys.* **247,** L25–L27.

Paresce, F., and C. Burrows 1987, Broad-band imaging of the Beta Pictoris circumstellar disk. *Astrophys. J.* **319,** L23–L25.

Roques, F., H. Scholl, B. Sicardy, and B. Smith 1994. Is there a planet around β Pictoris? Perturbations of a planet on a circumstellar dusk disk. 1. The numerical model. *Icarus* **108,** 37–58.

Smith, B. A., and R. J. Terrile 1984. A circumstellar disk around β Pictoris. *Science* **226,** 1421–1424.

THOMAS, F., AND A. MORBIDELLI 1995. The Kozai resonance in the outer solar system and the dynamics of long-period comets. *Celest. Mech. Dynam. Astron.* submitted.

VIDAL-MADJAR, A., A.-M. LAGRANGE-HENRI, P. D. FELDMAN, H. BEUST, J. J. LISSAUER, M. DELEUIL, R. FERLET, C. GRY, L. M. HOBBS, M. A. MCGRATH, J. B. MCPHATE, AND H. W. MOOS 1994. HST-GHRS observations of β Pictoris: Additional evidence for infalling comets. *Astron. Astrophys.* **290,** 245–258.

WETHERILL, G. W. 1994. Possible consequences of absence of "Jupiters" in planetary systems. In *Planetary Systems: Formation, Evolution, Detection* (B. Burke, B. Rahe and J. Roettger, Eds.), pp. 23–32. Kluwer Academic, Dordrecht/Norwell, MA.

YOSHIKAWA, M. 1987. A simple analytical model for the ν_6 resonance. *Celest. Mech. Dynam. Astron.* **40,** 233–272.

YOSHIKAWA, M. 1989. A survey on the motion of asteroids in commensurabilities with Jupiter. *Astron. Astrophys.* **213,** 436–458.